Supporting Information

Stimuli-Responsive Small-on-Large Nanoradiosensitizer for Enhanced Tumor Penetration and Radiotherapy Sensitization

Wenhui Fu,[†,‡,⁄⁄,#] Xiao Zhang,[‡,⁄⁄,#] Linqiang Mei,[‡,§] Ruyi Zhou,[‡] Wenyan Yin,[‡,⁄⁄,*] Qiang Wang,[†,⁄⁄,*] Zhanjun Gu,[‡,§,*] Yuliang Zhao[‡,§]

[†] *Laboratory for Micro-sized Functional Materials, Department of Chemistry and College of Elementary Education, Capital Normal University, Beijing 100048, China*

[‡] *CAS Key Laboratory for Biomedical Effects of Nanomaterials and Nanosafety, Institute of High Energy Physics and National Center for Nanoscience and Technology, Chinese Academy of Sciences, Beijing 100049, China*

[⁄⁄] *CAS Key Laboratory of Nano-Bio Interface, Suzhou Institute of Nano-Tech and Nano-Bionics, Chinese Academy of Sciences, Suzhou 215123,China*

[§] *Center of Materials Science and Optoelectronics Engineering, College of Materials Science and Optoelectronic Technology, University of Chinese Academy of Sciences, Beijing 100049, China*

[#] *These authors contributed equally to this work.*

***** *Corresponding authors: yinwy@ihep.ac.cn, qwchem@gmail.com, zjgu@ihep.ac.cn*

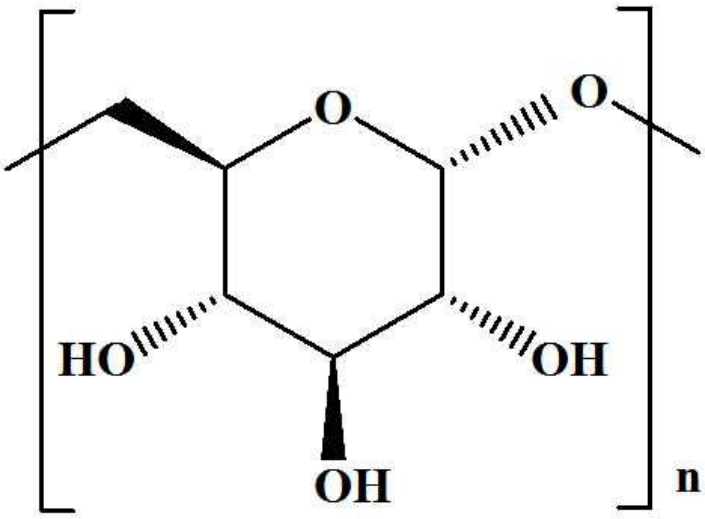

Figure S1. Structural formula of dextran.

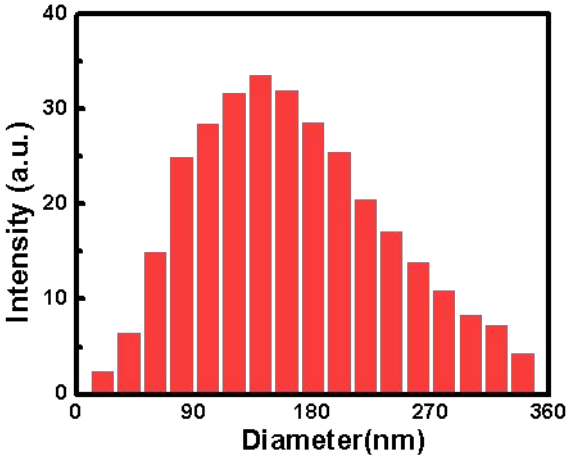

Figure S2. Hydrodynamic diameter of M/H-D.

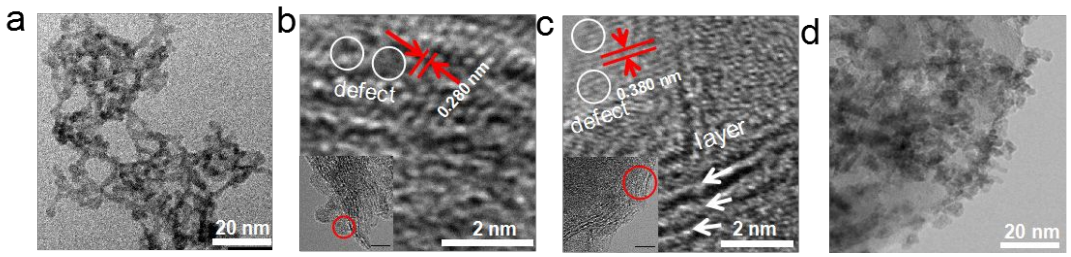

Figure S3. (a) TEM image of HfO_2 NPs. HRTEM and TEM (inset) images of (b) HfO_2 and (c) MoS_2 in M/H-D. Red circles in inset of (b) and (c) were the corresponding enlarged areas of the HRTEM images. White circles in (b) and (c) were the defects of the HfO_2 and MoS_2 in M/H-D. White arrows in (c) represented the layer of MoS_2. (d) TEM image of M/H-D after increasing the amount of $HfCl_4$ in the synthesis process.

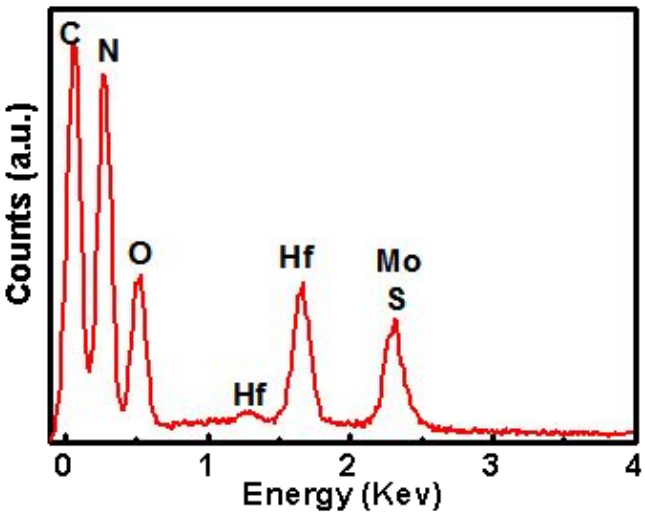

Figure S4. EDX of M/H-D.

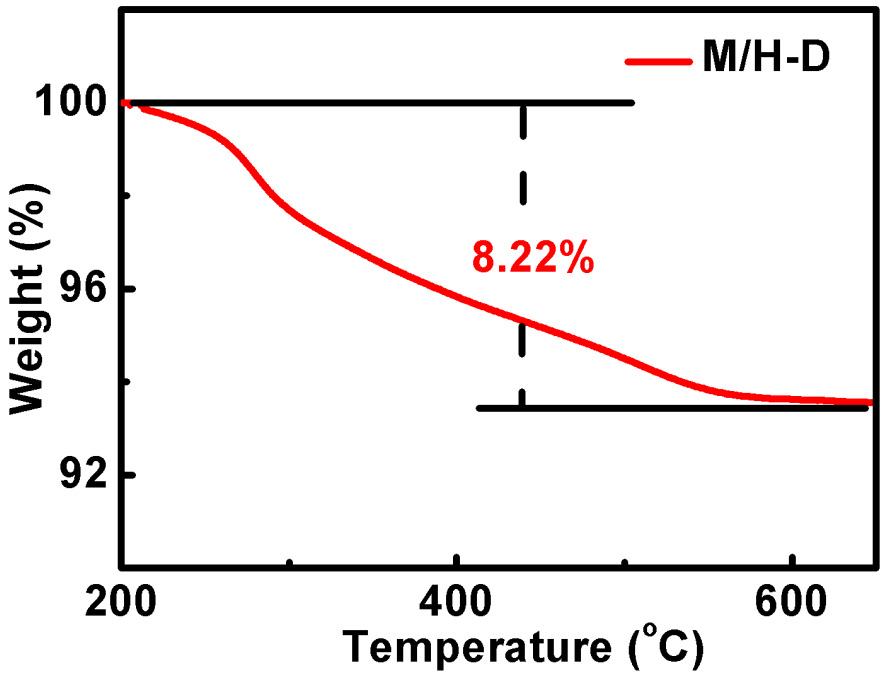

Figure S5. TGA analysis of M/H-D.

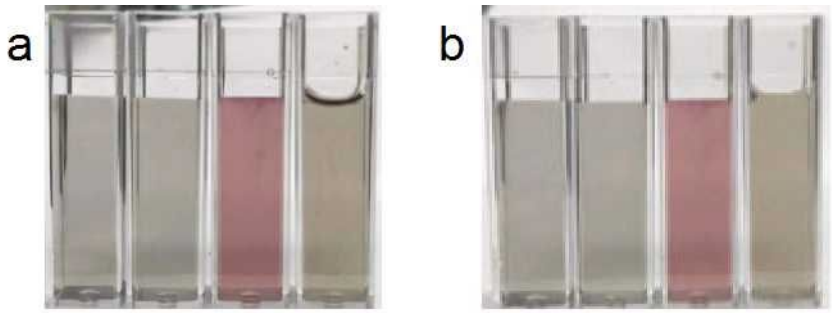

Figure S6. Photographs of 50 μg mL^{-1} of M/H-D dispersed in (from left to right) water, PBS, RPMI-1640 culture, and FBS at (a) 0 h (b) and 24 h at room temperature (25 ^{o}C).

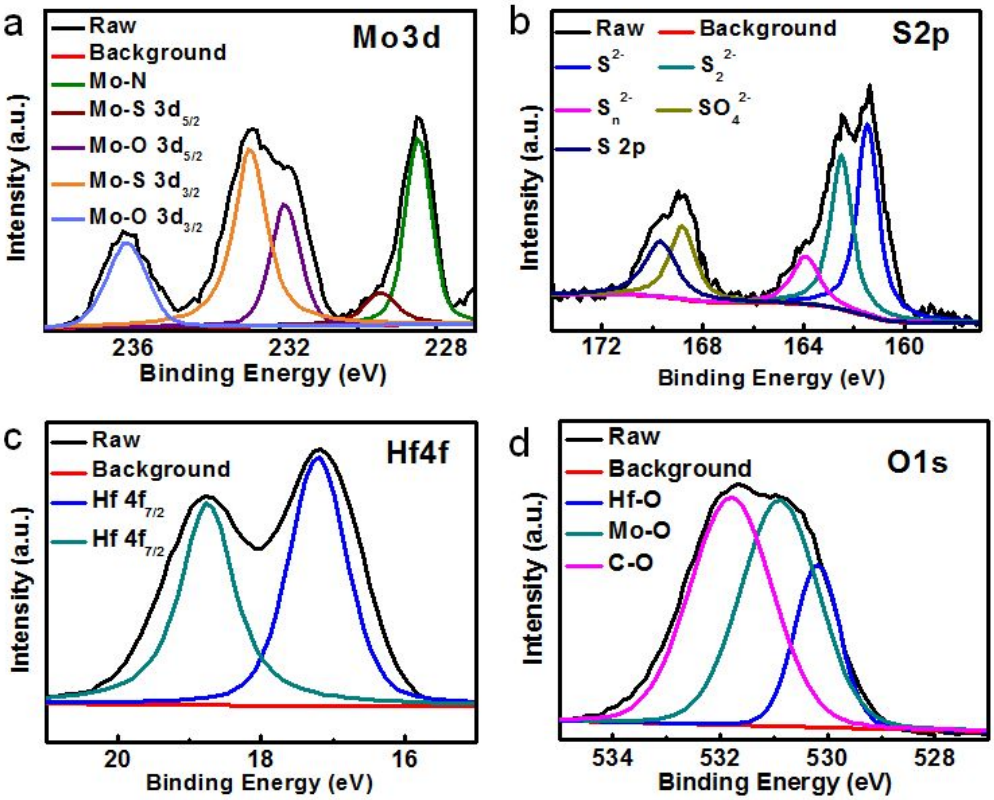

Figure S7. XPS survey spectra of M/H-D. (a) Mo, (b) S, (c) Hf, and (d) O elements and their corresponding fitting curves.

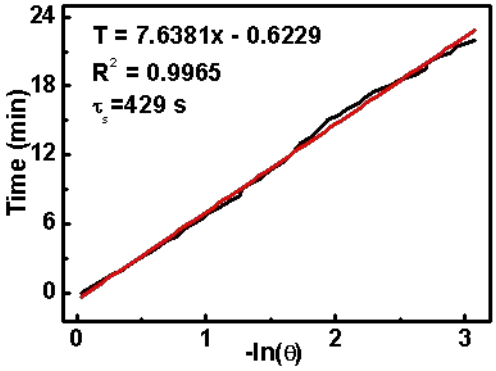

Figure S8. Linear time data *versus* -ln(θ) obtained from the cooling period.

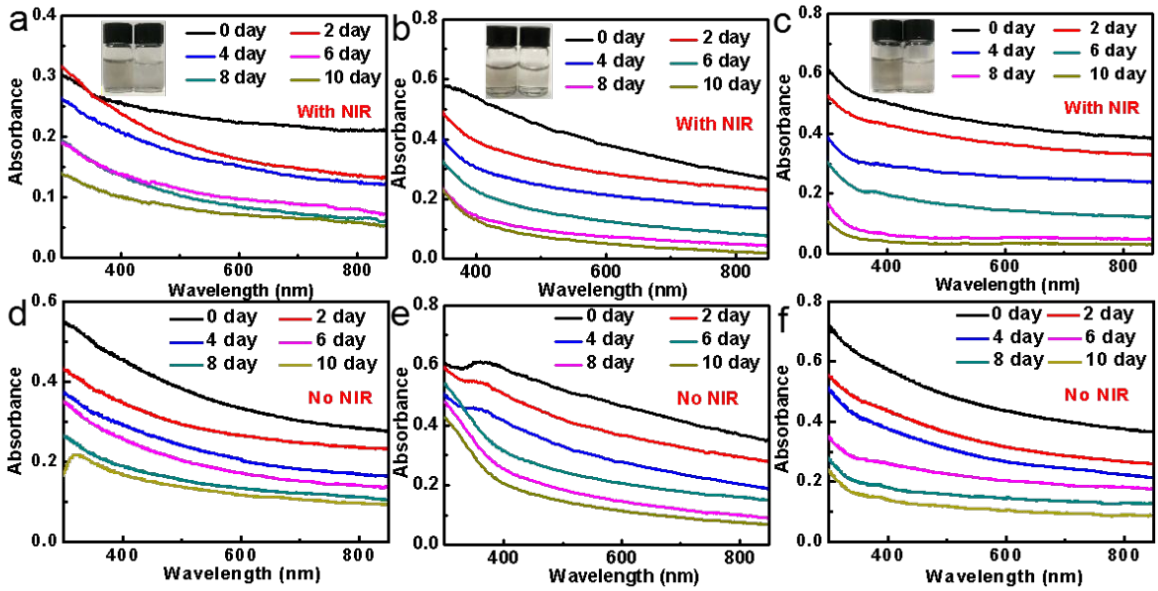

Figure S9. Biodegradation behaviors of the M/H-D in physiological concentration H_2O_2-pretreated SBF, STME, and SLF with/without NIR irradiation (5 min, 1.0 W cm^{-2}), corresponding to the results in Figure 2e. UV-Vis-NIR absorption spectra of M/H-D in (a) SBF with NIR, (b) STEM with NIR, (c) SLF with NIR, (d) SBF without NIR, (e) STEM without NIR, and (f) SLF without NIR irradiation. Inset: The color change photographs of biodegradable M/H-D (from left to right: 0 day and 10 day).

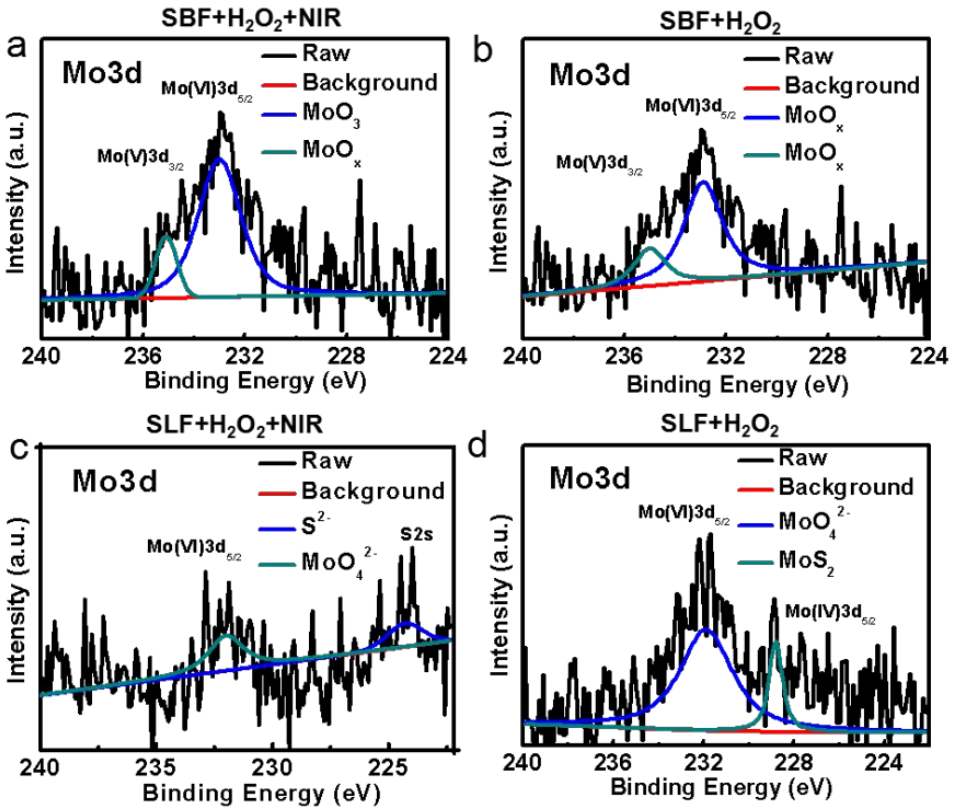

Figure S10. High-resolution Mo3d XPS core-level spectra of M/H-D with different treatments.

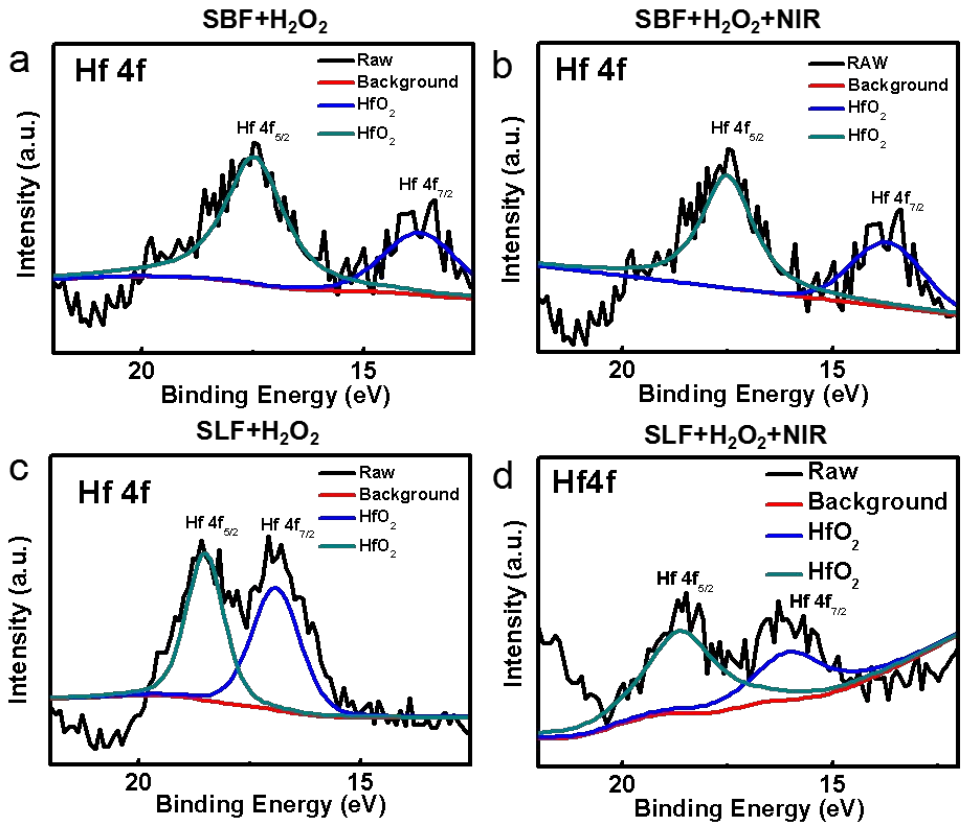

Figure S11. High-resolution Hf4f XPS core-level spectra of M/H-D with different treatments.

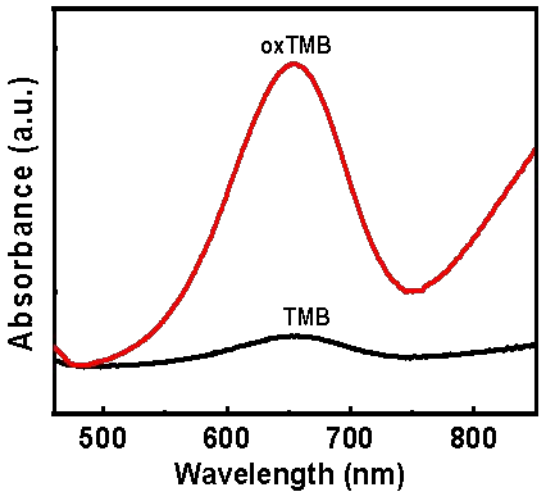

Figure S12. (a) Absorption spectra of TMB and oxTMB (reaction product of TMB). M/H-D: 50 μg mL^{-1}, TMB: 1.0 mM, H_2O_2: 100 μM. pH = 5.0, Temperature = 37 °C.

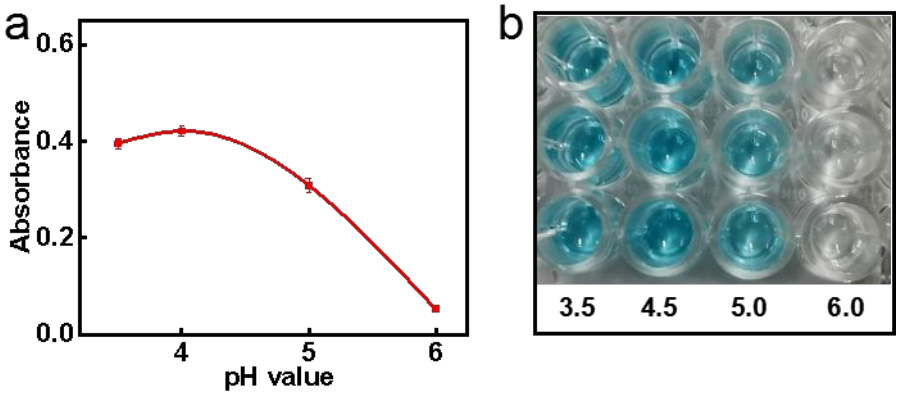

Figure S13. (a) The absorbance curve of oxTMB in the presence of H_2O_2 using M/H-D as peroxidase mimics, and TMB as a chromogenic substrate at different pH values. (b) Corresponding photos of colored solutions in (a). Concentrations of TMB: 1.0 mM, M/H-D: 50 μg mL^{-1}, H_2O_2: 100 μM, Temperature: 37 ^oC. Data represent mean ± standard error of the mean (n = 3).

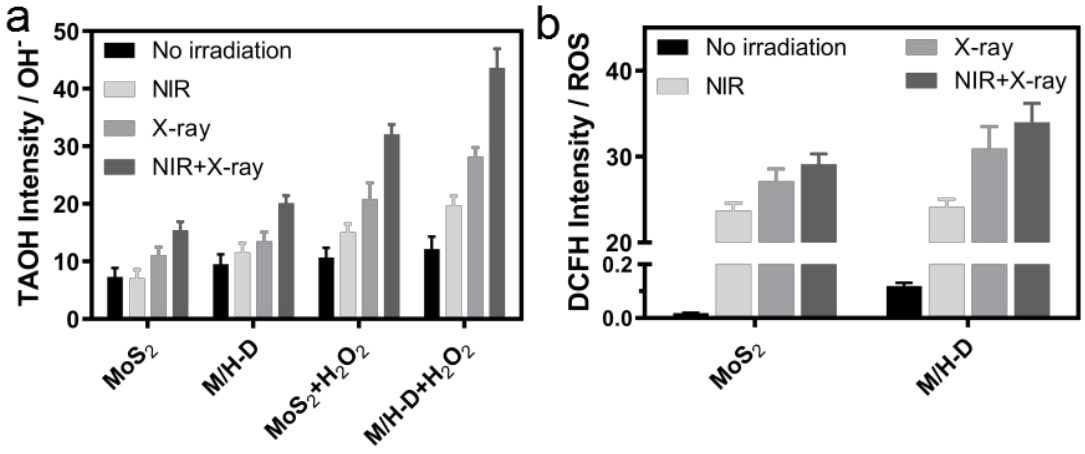

Figure 14. (a) Fluorescence enhancing ratio of TAOH after different treatments. Concentrations of M/H-D and MoS_2: 1.0 μg mL^{-1}. (b) Fluorescence enhancing ratio of DCFH-DA mixing with M/H-D or MoS_2 after different treatments. Data represent mean ± the standard error of the mean (n = 3). Concentrations of M/H-D and MoS_2: 10.0 μg mL^{-1}. X-ray: 50 kV, 75 μA, 10 min; NIR: 1.0 W cm^{-2}, 10 min.

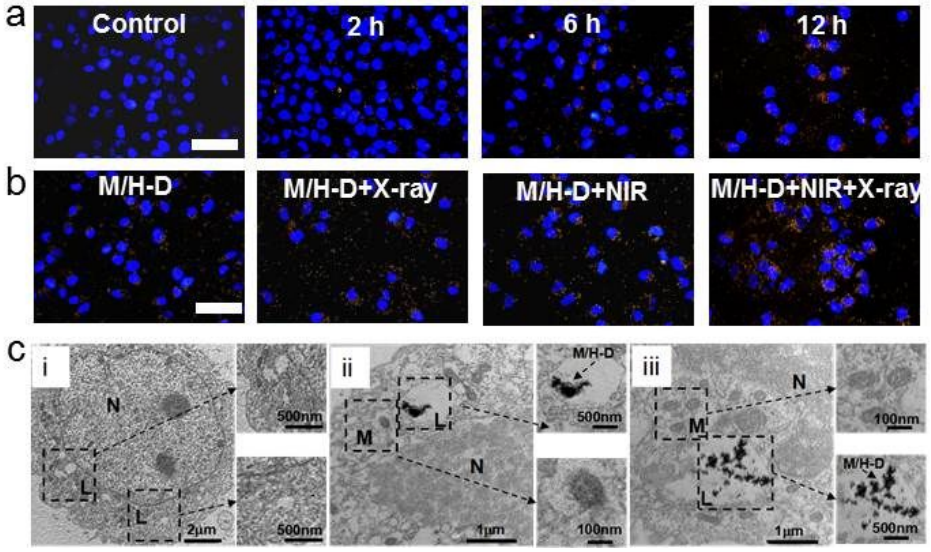

Figure S15. Dark-field scattering images of SMMC-7721 treated by M/H-D with different incubation time (a), and the images of SMMC-7721 treated with M/H-D, M/H-D + NIR, M/H-D + X-ray, and M/H-D + NIR + X-ray (b) (M/H-D: 100 μg mL^{-1}; Cellular uptake time: 6 h). The scale bar is 20 μm. Bio-TEM images of SMMC-7721 cells incubated (i) without or (ii) with M/H-D. (iii) Bio-TEM image of SMMC-7721 cells incubated with M/H-D irradiated by NIR plus X-ray (c). The N, M, and L represented nucleus, mitochondria and lysosomes respectively (M/H-D: 100 μg mL^{-1}, Cellular uptake time: 6 h; X-ray: 50 kV, 75 μA, 10 min; NIR: 1.0 W cm^{-2}, 10 min).

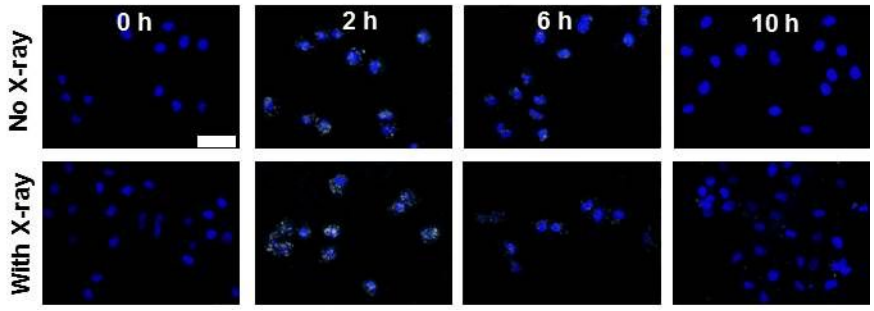

Figure S16. Dark-field scattering images of SMMC-7721 treated by HfO_2-D NPs in the absence or presence of X-ray (HfO_2: 100 μg mL^{-1}, X-ray: 50 kV, 75 μA). The scale bar is 20 μm.

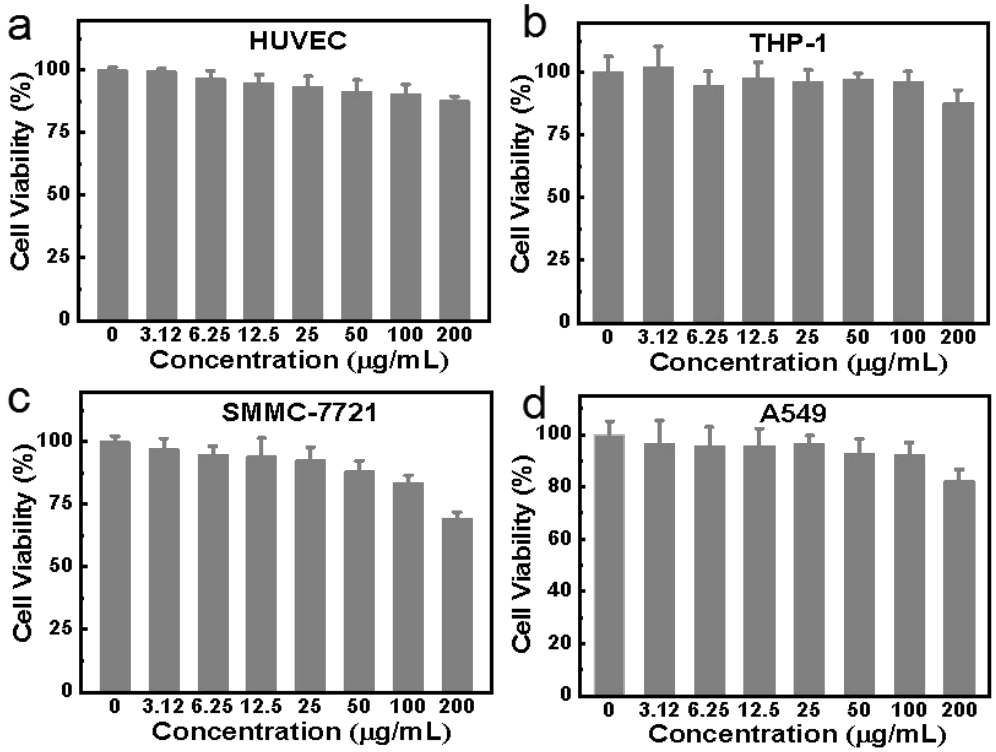

Figure S17. Cell viabilities of (a) HUVEC, (b) THP-1, (c) SMMC-7721, (d) A549 cells treated with different concentrations of M/H-D for 24 h. Data represent mean ± standard error of the mean (n = 6).

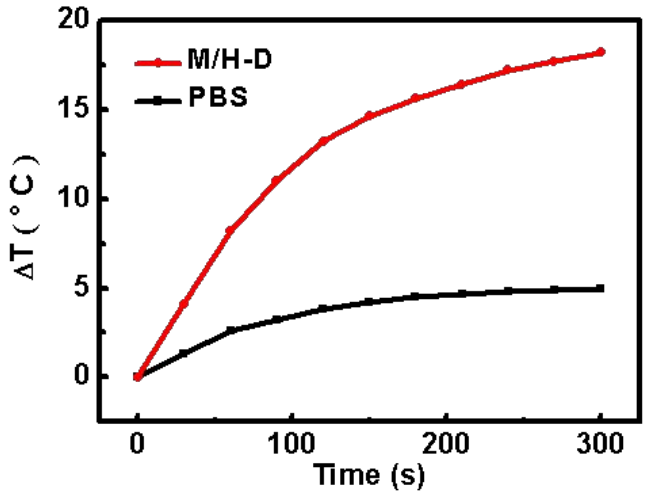

Figure S18. Temperature changes of tumor sites during NIR laser irradiation.

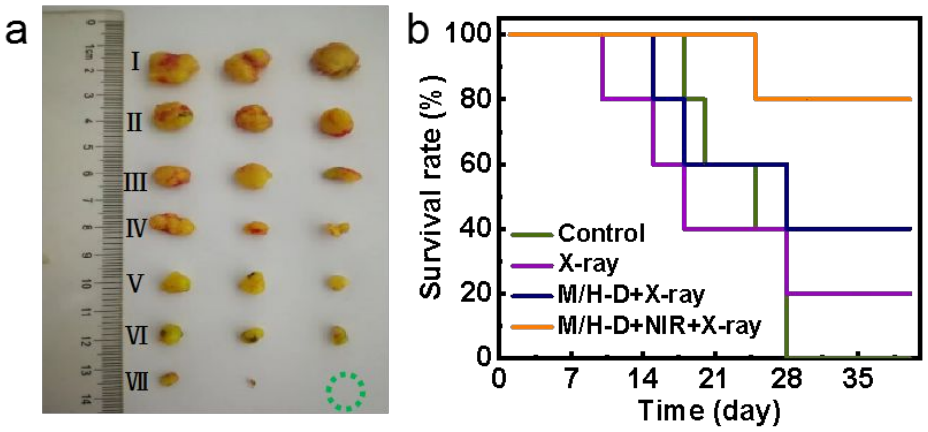

Figure S19. (a) Photograph of tumors treated with (I) PBS, (II) NIR, (III) X-ray, (IV) M/H-D, (V) M/H-D + NIR, (VI) M/H-D + X-ray, and (VII) M/H-D + NIR + X-ray. (b) Survival results of tumor therapy with different groups (five mice for each group).

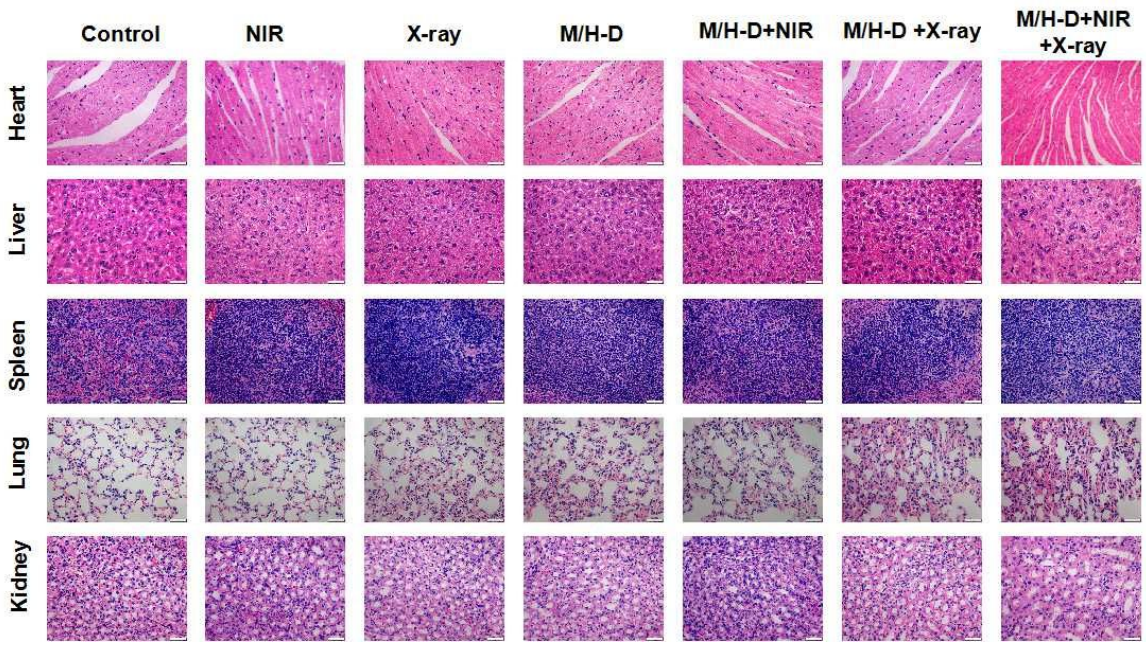

Figure S20. Representative H&E stained images of the main organs collected from tumor-bearing mice after different treatments within 28 days.

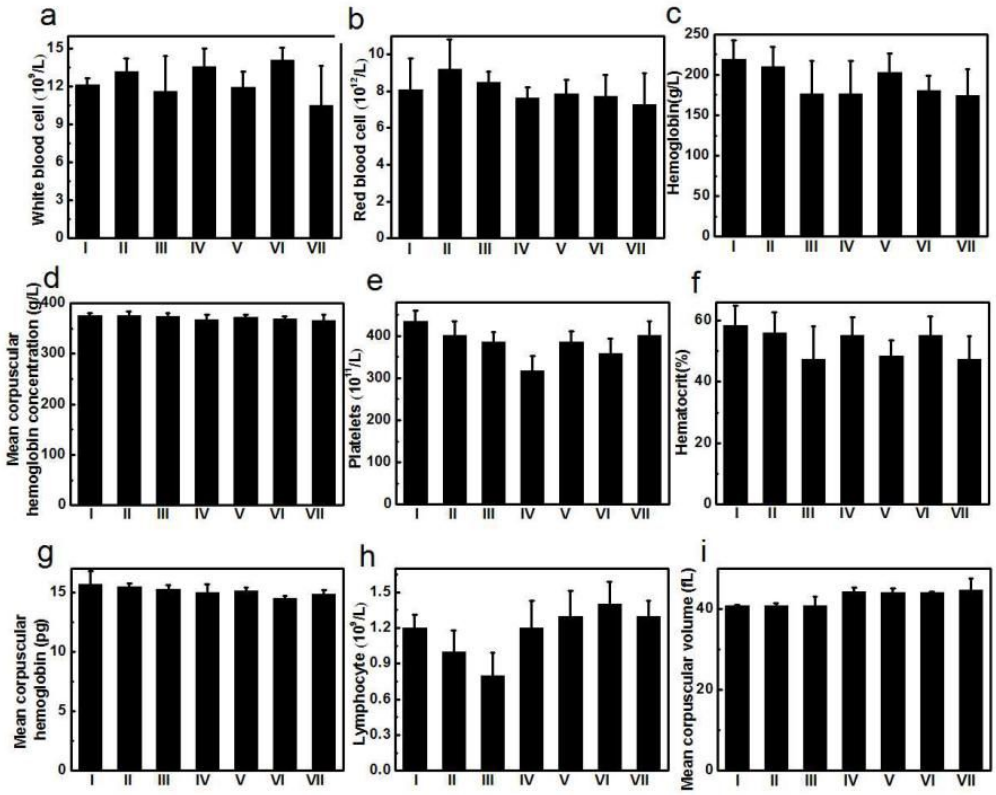

Figure S21. Blood biochemistry analysis of the mice at the last day. The results show the (a) white blood cell (WBC), (b) red blood cell (RBC), (c) hemoglobin (HGB), (d) mean corpuscular hemoglobin concentration (MCHC), (e) platelets (PLT), (f) hematocrit (HCT), (g) mean corpuscular hemoglobin (MCH), (h) lymphocyte (LYM) and (i) mean corpuscular volume (MCV) in each group. (I) PBS, (II) NIR, (III) X-ray, (IV) M/H-D, (V) M/H-D + NIR, (VI) M/H-D + X-ray, and (VII) M/H-D + NIR + X-ray. (All data represent mean ± standard error of the mean (n = 3))

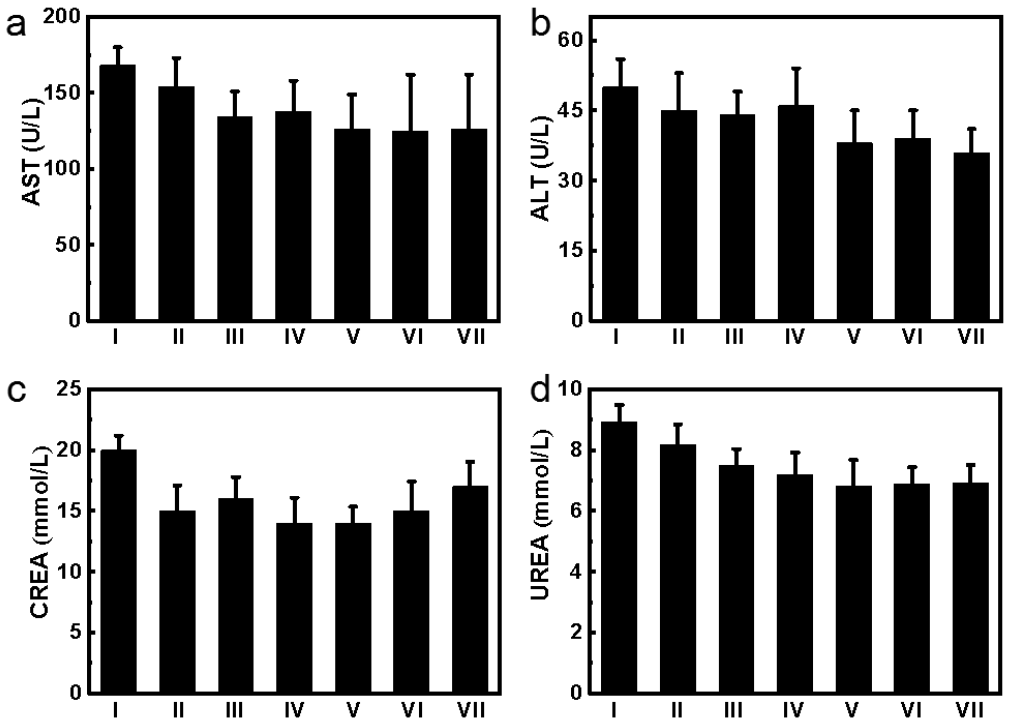

Figure S22. Blood biochemistry analyses of mice at the last day. The liver function was examined with (a) aspartate aminotransferase (AST) and (b) alanine aminotransferase (ALT). The kidney function was examined with (c) creatinine (CREA) and (d) urea (UREA). (I) PBS, (II) NIR, (III) X-ray, (IV) M/H-D, (V) M/H-D + NIR, (VI) M/H-D + X-ray, and (VII) M/H-D + NIR + X-ray. (All data represent mean ± standard error of the mean (n = 3))

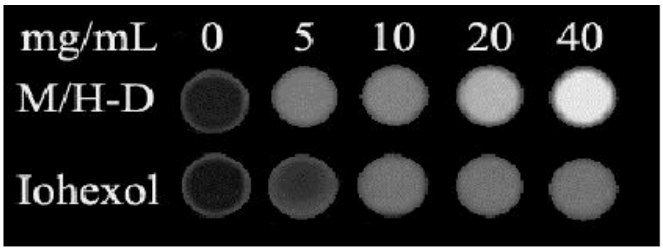

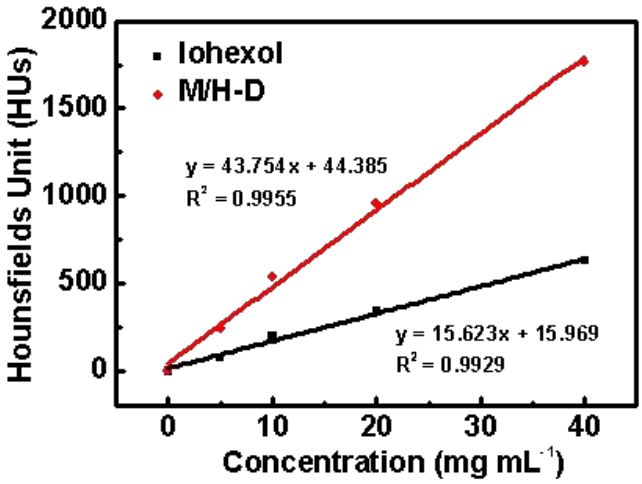

Figure S23. CT values of the Iohexol and M/H-D with different concentrations and corresponding HU values.

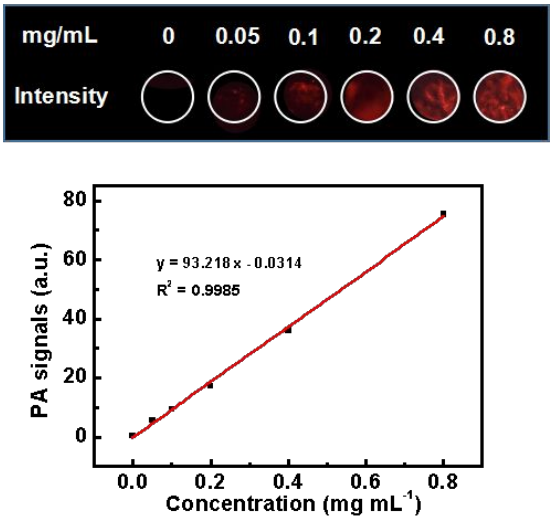

Figure S24. *In vitro* PAT signals intensity of the M/H-D with different concentrations.

Table S1. The detailed parameters of all the *in-vitro* irradiation experiments.

Type	Voltage (kV)	Current (μA)	Distance (cm)	Time (min)	Dose rate (Sv h^{-1})
DNA Damage	50	75	3	10	100
Colony Formation Assays	50	75	3	0.5~2	100
Cellular Uptake	50	75	3	10	100
ROS Detection in Cells	50	75	3	10	100
ROS and ·OH Detection	50	75	1	10	200
Bio - TEM	50	75	3	10	100